How ferrocyanide influences NaCl crystallization under different humidity conditions

CRYSTAL GROWTH & DESIGN

Article

pubs.acs.org/crystal

How Ferrocyanide Influences NaCl Crystallization under Different Humidity Conditions

Sonia Gupta, Hendrik P. Huinink,* Leo Pel, and Klass Kopinga

Transport in Permeable Media, Department of Applied Physics, Eindhoven University of Technology, P.O. Box 513 5600 MB Eindhoven, The Netherlands

ABSTRACT: The effect of ferrocyanide ions on moisture/ion transport and salt crystallization processes in salinated porous materials under different environmental conditions has been studied. A nuclear magnetic resonance (NMR) technique has been used for carrying out nondestructive, quantitative, and simultaneous measurements of both the hydrogen and sodium ion content. For salt saturated bricks without inhibitor, the slowest drying rate was observed at low relative humidity (0%). This is due to the blockage of pores near the drying surface that reduces the effective surface area available for evaporation. At high humidity (55% and 70%), due to low evaporative flux at the surface, the drying front is located on the surface of the material. Because of this, salt crystallizes as efflorescence, and blockage effects were less significant and consequently the drying rate was higher. With the addition of inhibitor at low relative humidity, due to distinct crystal morphology, salt crystallizes as efflorescence, and the saturation concentration was attained very slowly inside the brick. At higher relative humidity, in the presence of inhibitor no significant difference either in the amount of efflorescence formed or the speed at which the saturation concentration was attained inside the brick was found. These results show that the use of inhibitor will be beneficial in the environment that promotes faster drying such as low relative humidity, high temperature, etc. For such cases, inhibitor can convert subflorescence to efflorescence and can thus reduce salt damage.

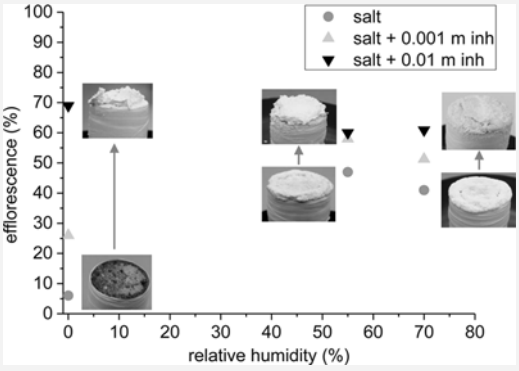

1. INTRODUCTION

Salt weathering leads to the destruction of many valuable cultural heritage monuments and porous building materials. Soluble salts such as chlorides, sulphates, and nitrates are known to be the reason behind damage. Among the various salts commonly found in buildings, sodium chloride (NaCl) is one of the most abundant and ubiquitous. The damage of the porous materials is mainly due to the growth of salt crystals inside the porous matrix of the materials. The growth of salt crystals exerts pressure on the pore walls, which can exceed the tensile strength of the materials causing damage.[1] To prevent or reduce the structural damage of the materials, an effective and practically feasible method is required. The use of crystallization inhibitors has been proposed as a potential preventive treatment method. These inhibitors act either by preventing or by delaying the onset of nucleation[2] (and hence crystallization) or by changing the crystal growth mechanism by adsorbing onto specific crystal faces.[3] Their application in the field of architectural conservation is not yet fully explored. The use of ferrocyanide (FC) ions as a preventive measure against NaCl damage has been proposed in the past.[4,5] These compounds are known to promote the formation of efflorescence rather than subflorescence.[4,5] Because of the formation of efflorescence, the amount of salt crystallized inside the material decreases. It is known that efflorescence changes the drying kinetics of porous media by changing the boundary conditions near material/air interface.[6] Eloukabi et al.[7] have reported two types of efflorescence: crusty efflorescence, when a salt crystal crust forms at the surface of the porous medium and severely limits the evaporation rate, and patchy efflorescence, when the evaporation is not significantly limited by the presence of the crystallized salt at the surface of the porous medium. The evaporation rate can be in fact even greater than with pure water owing to the enhanced evaporation surface.[7] Consequently, efflorescence contributes significantly in changing the drying behavior of porous materials.

For bulk solutions, in the presence of inhibitor increased supersaturation levels have been reported in the past.[8] However, it is important to see the effect of these compounds on the concentration of NaCl solutions inside a porous media. It is known that the process behind the damage due to salt crystallization is the growth of salt crystals in confined spaces (e.g., pores), hence exerting crystallization pressure on the pore walls. Thermodynamically, for an anhydrous salt the crystallization pressure (P_c) can be related to supersaturation (C/C_o) of the solution as[9]

Received: October 17, 2013
Revised: February 7, 2014
Published: February 19, 2014

$$P_c = \frac{\nu RT}{V_m} \ln\left(\frac{C}{C_o}\right) \quad (1)$$

where ν is the total number of ions released upon dissociation of the salt (e.g., for NaCl = 2), R is the universal gas constant, T is the absolute temperature, V_m is the molar volume of the salt crystal, C and C_o are the actual concentration and the saturation concentration of salt, respectively. Hence, if inhibitor brings supersaturation inside a porous material, it can cause damage to the material. However, recently, a study has been performed on the influence of ferrocyanide ions on NaCl crystallization and moisture/ion transport phenomena inside a porous brick.[8] It was reported that the presence of inhibitor changes the drying conditions near the material/air interface due to a change in crystal morphology, and most of the dissolved salt ions crystallize as nondestructive efflorescence. No high supersaturation has been reported inside the material in the presence of inhibitor. Hence, it was concluded that the use of ferrocyanide ions against NaCl damage is effective. However, in that study drying tests were performed at 0% RH, whereas in practice the humidity can be much higher. Consequently, before using inhibitors to treat a historic object there is an urgent need to assess the effectiveness of their application at different environmental conditions.

The aim of the study reported in this paper is to understand the drying and crystallization behavior of NaCl saturated porous materials in the presence of inhibitor at different relative humidity conditions. Using a specially designed nuclear magnetic resonance (NMR) setup,[10] the salt ion concentration was measured directly, nondestructively, inside a real porous material. In the past, an in situ studies of the supersaturation at the onset of crystallization within porous media have been performed.[11−13] However, using NMR,[10] we can measure both the hydrogen and sodium ion profiles simultaneously during dynamic drying experiments. From the ratio of the local sodium and hydrogen content, the time evolution of the salt ion concentration inside the porous material can be determined as a function of position.

2. THEORY

Drying of a porous material occurs due to the humidity gradient between the air/material interface and the environment. The water vapor moves away from the surface, thereby causing drying of the brick. The rate of volume change of water dV/dt (m^3 s^{-1}) across the material/air interface under isothermal conditions is given by the Fick's law:

$$\frac{dV}{dt} = D\frac{A}{\rho}\frac{M}{RT}\frac{(P_i - P^*)}{\delta} \quad (2)$$

where A (m^2) is the effective surface area available for evaporation, ρ (g m^{-3}) is the density of liquid water, D (m^2 s^{-1}) is the diffusivity of water vapor in air, M (g mol^{-1}) is the molar mass of water, R (J mol^{-1} K^{-1}) is the gas constant, T (K) is the temperature, P_i and P^* (N m^{-2}) are the water vapor pressures at the air/water interface at the material surface and in the surrounding air respectively, and δ (m) is the thickness of the boundary layer through which the diffusion of water vapor takes place. Therefore, at a constant temperature the drying rate mainly depends on the difference between the water vapor pressures at the interface and the environment (i.e., the relative humidity gradient), the effective area available for evaporation, and the air flow that determines the thickness of the boundary layer δ. So, for a given material at a given air flow, drying should be proportional to the relative humidity gradient. This holds true only in the first phase of drying when there is a continuous network of liquid inside the material to meet the demands of evaporative flux at the surface. During this stage, the rate of evaporation is controlled by external conditions rather than by the rate of transport within the material.

For a water saturated brick, the air in direct contact with water at the air/water interface is saturated with water vapor, and therefore, $P_i = P_{sat}$, where P_{sat} is the saturated vapor pressure of the liquids having planar surfaces. For the curved surfaces, for example, in capillaries and drop, the saturated water vapor pressure changes. The Kelvin equation tells us how the saturated vapor pressure depends on the curvature of the liquid. For cylindrical capillaries of radius r, Kelvin equation is given as

$$\ln\left(\frac{P_i}{P_{sat}}\right) = \frac{\gamma}{r}\frac{V_m}{RT} \quad (3)$$

where γ (N m^{-1}) is the surface tension, V_m (m^3 mol^{-1}) is the molar volume of the liquid, and r (m) is the radius. However, in the case of a fired-clay brick, the pore sizes are in the range of 1−10 μm.[8] So, the influence of the capillary pressure on P_i is negligible, So, P_i can be taken as equal to P_{sat} in eq 2. However, for the materials with smaller pore sizes on the order of nanometers, this effect should be kept in mind.

The location of salt crystallization in a material is determined by the competition of two mechanisms: diffusion and advection. Advection leads to an accumulation of salt ions near the surface, thus increasing the local salt ion concentration in this region. The surface accumulation leads to a concentration gradient within the material, which in turn induces diffusion to level off the concentration gradient. The competition between advection and diffusion is generally written in terms of a Peclet number:[14]

$$\mathrm{Pe} = \frac{|U|L}{D_{eff}} \quad (4)$$

where U (m s^{-1}) is the fluid velocity, L (m) is the length of the sample, and D_{eff} (m^2 s^{-1}) is the effective diffusion coefficient of the salt ions in a material and is given by τD, where τ is the tortuosity and D is the diffusion coefficient. Initially, the evaporative flux at the drying surface is balanced by the liquid flow due to capillary action; thus an average value of fluid velocity can be estimated by using $J/\varphi\rho$ where, J (kg m^{-2} s^{-1}) is the average mass flux, φ is the porosity of the material, and ρ (kg m^{-3}) is the density of water. For Pe < 1, diffusion dominates and for Pe > 1, advection dominates.

3. EXPERIMENTAL SECTION

3.1. Nuclear Magnetic Resonance (NMR). In this study, NMR is used for carrying out nondestructive, quantitative, and simultaneous measurement of both hydrogen and sodium ion content in the sample during dynamic drying experiments. From the ratio of local sodium and hydrogen content, the salt ion concentration inside the porous material can be determined. For the experiments presented here, a home-built NMR scanner with a static magnetic field of 0.78 T and gradient up to 0.3 T m^{-1} was used.[10] The details of the setup and the parameters used for the experiments can be found elsewhere.[8,10,15]

3.2. Materials. All the tests have been performed on a fired-clay brick. The measured average porosity (water immersion method) was 0.32 m^3 m^{-3}. The pore size distribution was determined by mercury intrusion porosimetry (MIP). It ranges from 1 to 10 μm (accounting

for ~80% of the total pore space).[8] Potassium hexa-cyanoferrate (II) trihydrate $K_4[Fe(CN)_6]\cdot 3H_2O$ was tested as a crystallization inhibitor.

3.3. Method. In this study, cylindrical brick samples of 20 mm diameter and 40 mm length were saturated with water, 3 m NaCl solution without inhibitor, and 3 m NaCl solution with inhibitor. Two concentrations of inhibitor (0.001 and 0.01 m) were tested. To avoid evaporation, the samples were sealed using a Teflon tape on all sides except the top surface. Afterward, the samples were placed inside NMR sample chamber for drying at a flow rate of 1 L min^{-1}. The relative humidity was varied at 0%, 55%, and 70%. All the experiments have been performed at room temperature. Using a step motor, the sample was moved in the vertical direction to allow the measurement of moisture and sodium content throughout the sample length. A schematic of the setup is given in our previous article.[8] At the end of each drying experiment, the efflorescence from the sample surface was collected and weighed.

4. RESULTS AND DISCUSSION

Our main focus was to understand the influence of inhibitor on the crystallization and drying behavior of salinated porous materials at different humidity conditions. For this purpose, initially the drying behavior of water and salt saturated material was studied at different humidity conditions.

4.1. Drying Behavior of Fired-Clay Brick Saturated with Water. First, the drying behavior of water saturated bricks at different relative humidity conditions was studied and compared. Typical moisture profiles of water saturated brick dried at 0% RH has been shown and discussed in our previous article.[8] In this work, the drying behavior of water saturated bricks at higher RH (55% and 70%) was studied and compared to the brick dried at 0% RH. Using NMR, the moisture profiles were recorded for the bricks dried at 55% and 70% RH. Instead of showing all those moisture profiles, the results from various experiments are given in Figure 1a, where the normalized integrated hydrogen signal (S_H) is plotted as a function of time (t). The integrated hydrogen signal at 0% RH has been calculated from the moisture profile data shown in ref 8. The integrated hydrogen signal at a given time represents the total amount of water in the brick. As can be seen in Figure 1a, the drying rate of water saturated bricks was slower at high relative humidity, which can be understood by considering the flux eq 2. As mentioned before for water saturated samples, the air in direct contact with water (at the air/water interface) is saturated with water vapor, and therefore $P_i = P_{sat}$ and $P^* = P_{sat} \times RH/100$, where RH is the relative humidity of the environment. With increasing environmental humidity, the water vapor pressure in the surrounding air also increases ($P^* = P_{sat}$ RH/100). This decreases the humidity gradient between the air/material interface and the surrounding air and slows down the drying.

To confirm if humidity is the only factor responsible for the observed decrease in drying rate, a scaling of the time axis was done. For this purpose, the time axis was multiplied by a scaling factor $(P_i - P^*)/P_{sat}$. The results are shown in Figure 1b, where the normalized integrated hydrogen signal is plotted as a function of $(P_i - P^*)/(P_{sat})t$. This figure shows that the drying curves of water saturated bricks dried under different relative humidity conditions coincide very well, especially at the initial stage of drying. This confirms that the decrease of the drying rate results from the depression of the humidity gradient only. The experimental value of δ is calculated in the beginning of drying using eq 2. The value of δ is found to be ~700 μm. The pore sizes in fired-clay brick are on the order of 1−10 μm, which is much smaller than the thickness of boundary layer (~700 μm). Therefore, an approximately homogeneous boundary layer can be assumed to be present at the surface of the material.

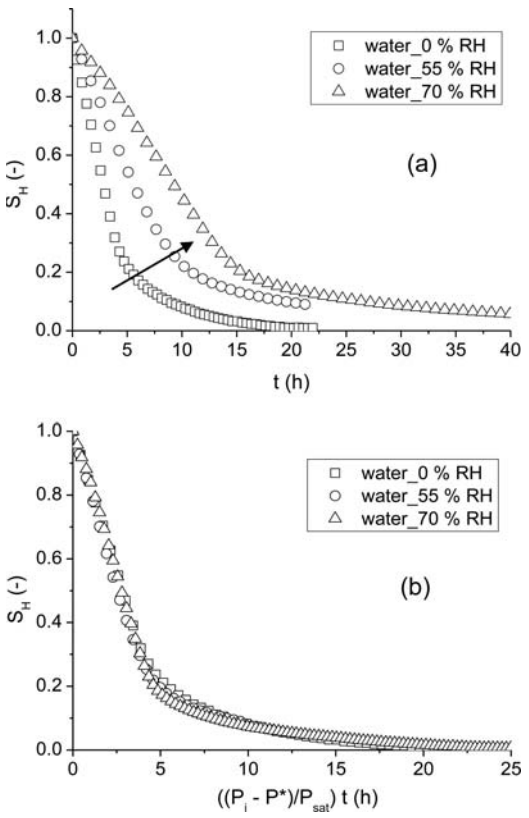

Figure 1. (a) Normalized integrated hydrogen signal (S_H) as a function of time (t) for water saturated fired-clay bricks dried at different relative humidity conditions. The integrated hydrogen signal at 0% RH was calculated from the moisture profile data shown in our previous work.[8] (b) Normalized integrated hydrogen signal (S_H) as a function of the scaled time $(P_i - P^*)/(P_{sat})t$. P_i, P^*, and P_{sat} are the water vapor pressures at the air/water interface at the material surface, in the surrounding air and saturation vapor pressure of the liquid respectively.

4.2. Drying and Crystallization Behavior of Salt Saturated Fired-Clay Brick without Inhibitor. To understand the drying and the crystallization behavior of bricks in the presence of salt, the samples were saturated with 3 m NaCl solution and were dried at different relative humidity conditions.

Drying Behavior of Salt Saturated Fired-Clay Brick at Different Relative Humidity Conditions. The drying behavior of salt solution saturated bricks was studied at high humidity conditions (55% and 70%) and was compared to the brick dried at 0% RH. The results are given in Figure 2a, where the normalized integrated hydrogen signal is plotted as a function of time. The integrated hydrogen signal for salt solution saturated brick dried at 0% RH has been calculated from the moisture profile data shown in our previous work.[8] The results show that the drying rate of salt saturated bricks is lower than that of water saturated bricks (compare the time scales in Figures 2a and 1a). The drying rate of a salt solution saturated brick at 0% relative humidity slows down dramatically (see Figure 2a) after approximately 15 h. At this time, the drying rate of the brick became even lower than that of the bricks dried at higher humidity. On the other hand, the drying rate of

dx.doi.org/10.1021/cg4015459 | Cryst. Growth Des. 2014, 14, 1591−1599

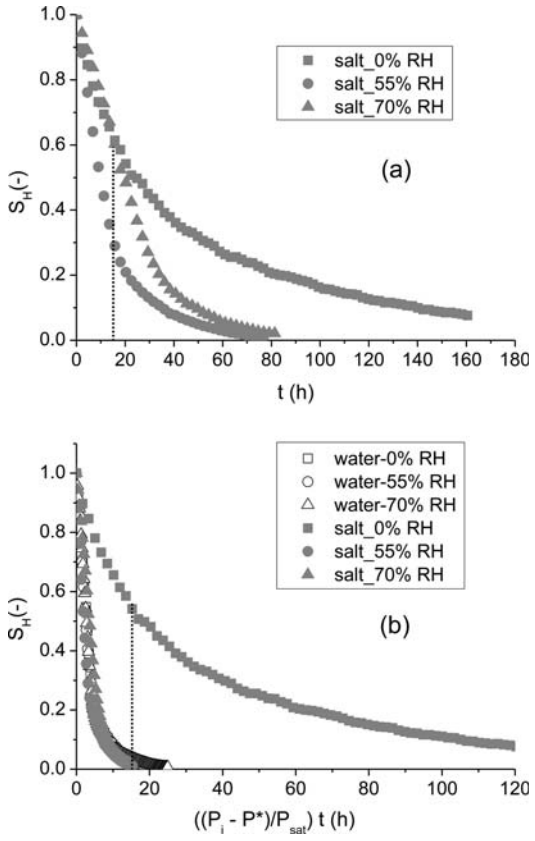

Figure 2. (a) Normalized integrated hydrogen signal (S_H) as a function of time (t) for salt loaded bricks dried at different relative humidity conditions. The integrated hydrogen signal at 0% RH has been calculated from the moisture profile data shown in our previous work.[8] (b) Normalized integrated hydrogen signal (S_H) as a function of the scaled time $(P_i - P^*)/(P_{sat})t$. P_i, P^*, and P_{sat} are the water vapor pressures at the air/water interface at the material surface, water vapor pressures in the surrounding air, and saturation vapor pressure of the liquid respectively.

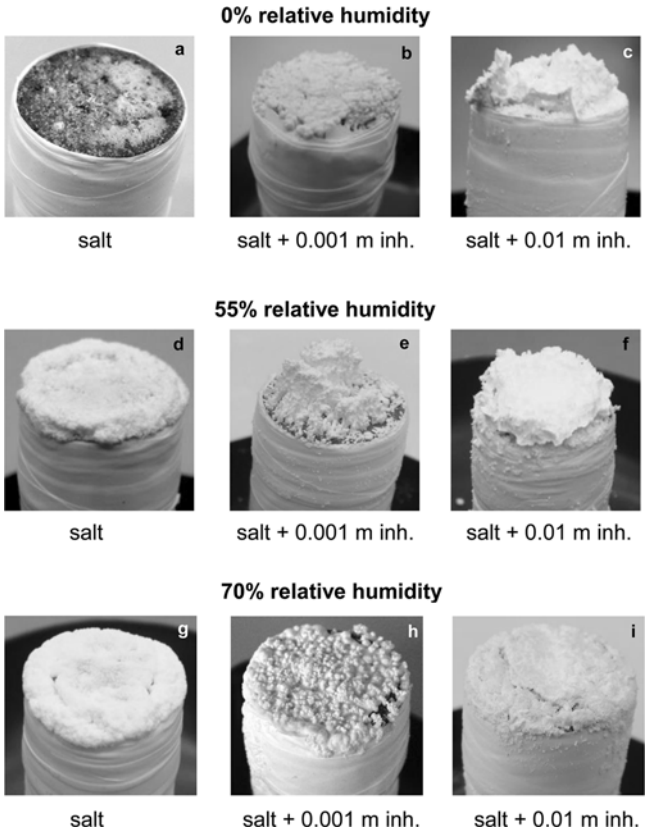

Figure 3. Pictures of the efflorescence formed at the end of the drying experiment in the case of salt saturated brick with and without inhibitor dried at 0% (3a, 3b, 3c), 55% (3d, 3e, 3f), and 70% (3g, 3h, 3i) RH. In the absence of inhibitor, the amount of efflorescence increases at higher humidity. At 0% RH, the amount of efflorescence increases significantly with the addition of inhibitor. At high humidity, a comparable amount of efflorescence was formed in both cases, that is, with and without inhibitor.

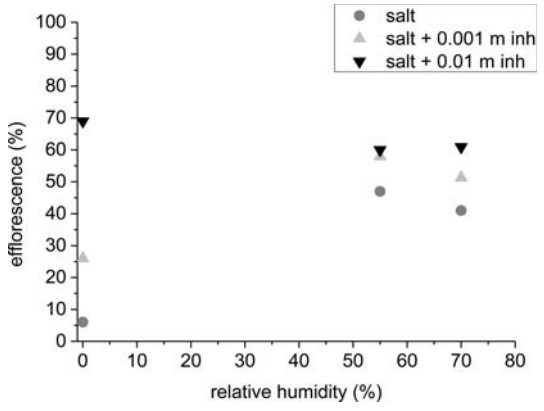

Figure 4. The percentage efflorescence formed during the drying experiment as a function of relative humidity for salt saturated bricks with and without inhibitor. The percentage efflorescence represents the ratio of the amount of salt crystallized as efflorescence and the initial amount of dissolved salt.

the brick dried at 70% RH was lower than that of the brick dried at 55% RH. In addition, a difference in the amount of efflorescence formed was seen. A negligible amount of salt crystallized as efflorescence at 0% RH in comparison to the amount of efflorescence formed at high humidity. Approximately 48% and 40% of salt crystallized as efflorescence at 55% and 70% RH respectively compared to 6% efflorescence formed at 0% RH. The pictures of the salt crystallized as efflorescence taken at the end of the experiments are shown in Figure 3, panels a, d, and g for the bricks dried at 0%, 55%, and 70% RH respectively. In Figure 3a, the preferential location of salt crystallization at the surface of the brick can be due the underlying porosity and permeability difference. These differences might promote solution flow at one location than the other. Quantitative data showing the percentage of salt crystallized as efflorescence are plotted as a function of relative humidity in Figure 4.

To check if depression of relative humidity gradient is the only factor responsible for the slow drying, a scaling of the time axis was done. The results are plotted in Figure 2b, where the normalized integrated hydrogen signal is plotted as a function of scaled time. For comparison, the results for both water and salt saturated samples are included in Figure 2b. Except for the brick dried at 0% RH, the drying curves coincide well, indicating that for 55% and 70% RH the decrease of the drying rate indeed results from the depression of the relative humidity gradient only. However, for the fired-clay brick dried at 0% RH, the drying rate was exceptionally lower.

The rates of initial volume change of the solution for water and salt saturated samples dried at different relative humidity

dx.doi.org/10.1021/cg4015459 | Cryst. Growth Des. 2014, 14, 1591−1599

conditions were compared. The results are given in Figure 5. The values of the volume change are obtained from the slope of

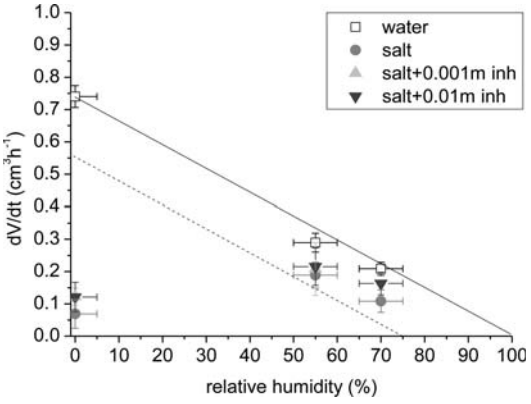

Figure 5. The rate of initial volume change of the solution (dV/dt) as a function of the relative humidity for the bricks saturated with water, salt and salt + inhibitor solution (see Figures 1a and 2a). The solid line and the dashed line represent a linear fit to the data where the flux gets zero, that is, at 100% for water saturated samples and at 75% for salt saturated samples. The values of the volume change are obtained from the slope of a straight line fitted to the time dependent integrated volume for stage 1 drying only. The solid line drawn through the values of volume change for water saturated samples is a guide to eye. For NaCl solution saturated samples, the flux should be zero at 75% RH. Considering this fact, a theoretical dashed line is drawn parallel to the solid line.

a straight line fitted to the time dependent integrated volume for stage 1 drying only. A linear fit is drawn through the values of volume change for water saturated samples. This line shows, as expected, a decrease of water vapor flux with increasing relative humidity, and the flux becomes zero at 100% RH. For NaCl solution saturated samples, the flux should be zero at 75% RH. Considering this fact, a theoretical dashed line is drawn parallel to the solid line for salt saturated samples. The values of the volume change for salt saturated samples should lie on this line, if the decrease in the drying rate results from the depression of the humidity gradient only. The figure shows that for samples dried at high relative humidity, that is, 55% and 70%, the values of volume change are close to the expected values. For the salt saturated brick dried at 0% RH, the initial volume change is exceptionally low. This clearly indicates that another mechanism is causing slow drying of the brick at 0% RH. This behavior can be understood from the observed salt efflorescence differences.

The observed drying behavior of the material is explained with the help of a schematic representation of the drying process shown in Figure 6. Figure 6a–c represents a schematic for water saturated brick, salt saturated brick dried at 0% RH, and salt saturated bricks dried at 55%/70% RH respectively. In these pictures, L is the length of sample, and δ (m) is the thickness of boundary layer through which the water vapor diffusion takes place. These figures show a simplistic picture of drying. However, for the case in which the evaporation flux is not uniform over the entire surface, the thickness of the mass boundary (δ) layer will not be homogeneous over the entire surface. In the case of water saturated brick, the whole surface is available for evaporation (shown by vertical arrows in Figure 6a). However, for salt saturated bricks dried at 0% RH, a part of the surface is blocked by salt crystallization. This can be understood by considering the Pe number. As a first approximation, the value of the salt diffusion coefficient is taken as equal to 1.3×10^{-9} m^2 s^{-1} assuming $D_{eff} = D$.[7] In reality, D_{eff} will be less than D (as the tortuosity will be less than 1), and therefore the Pe will be higher than the value estimated here. The average value of the flux is taken as equal to the theoretical value (see Figure 5, the theoretical value of the volume change is represented by a dashed line). At t = 0 h, the calculated value of the Pe is 46. Therefore, advection is dominant at the start of the experiment. Consequently, salt ions will be advected along with the moisture toward the drying surface, accumulate there, and eventually crystallize. These salt crystals will block the pores near the drying surface, as shown in Figure 6b. Because of this blockage, the effective surface area available for evaporation decreases (shown by vertical arrows) compared to the surface area available for evaporation for water saturated bricks (refer eq 2). Because for a salt saturated brick the rate of initial volume change was small (see Figure 5), we expect a rapid formation of a thin layer of salt crystals in the first few minutes, with a very low permeability near the drying surface. The thickness of this layer is obviously too small to be observed within our experimental resolution.

At high relative humidity, the evaporative flux at the surface of material is lower providing more time for the salt ions to migrate along with the moisture to the drying surface and crystallize as efflorescence. The calculated value of Peclet number ~16 and ~8.4 in the case of 55% and 70% RH respectively confirms advection, and hence the salt crystallizes as efflorescence. Efflorescence reduces blockage of the pores near the drying surface, keeping the system open for drying. Thus, no decrease in the drying rate was seen at high humidity. As in our results all the drying curves coincide well after RH scaling (see Figure 2b), we do not expect any other effect to play a significant role either in enhancing or in reducing drying rates.

Crystallization Behavior of Salt Saturated Fired-Clay Brick at Different Relative Humidity Conditions. After understanding the drying processes of salt saturated material, the concentration levels reached by NaCl solutions within porous media was determined. For this purpose, the data are plotted in a so-called efflorescence pathway diagram (EPD).[15] The details of EPD can be found elsewhere.[8,15] Here, we will briefly summarize this discussion. In an EPD, two extreme situations can be distinguished. In the first case, diffusion dominates i.e., Pe < 1, resulting in a homogeneous distribution of salt ions throughout the sample. For such a case, during drying the salt solution concentration will increase homogenously throughout the sample, until the saturation concentration is achieved. Once the saturation concentration is achieved, any further drying will cause crystallization, and the concentration will stay constant at saturation concentration. In the second case, advection dominates, that is, Pe > 1, and ions will be dragged along with the moisture flow toward the drying surface. Accumulation of ions beyond the saturation concentration will immediately result in crystallization on the surface as efflorescence. If the rate of crystallization is high enough, the dissolved salt ion concentration inside the material will remain almost constant at the initial concentration.

The EPD for salt saturated bricks dried at 0%, 55%, and 70% RH are shown in Figure 7, where the dissolved salt content is plotted as a function of normalized average moisture content (the data for 0% RH have been taken from our previous article[8]). At high humidity (55% and 70%), the boundary line Pe > 1 is followed in contrast to an in between pathway, that is,

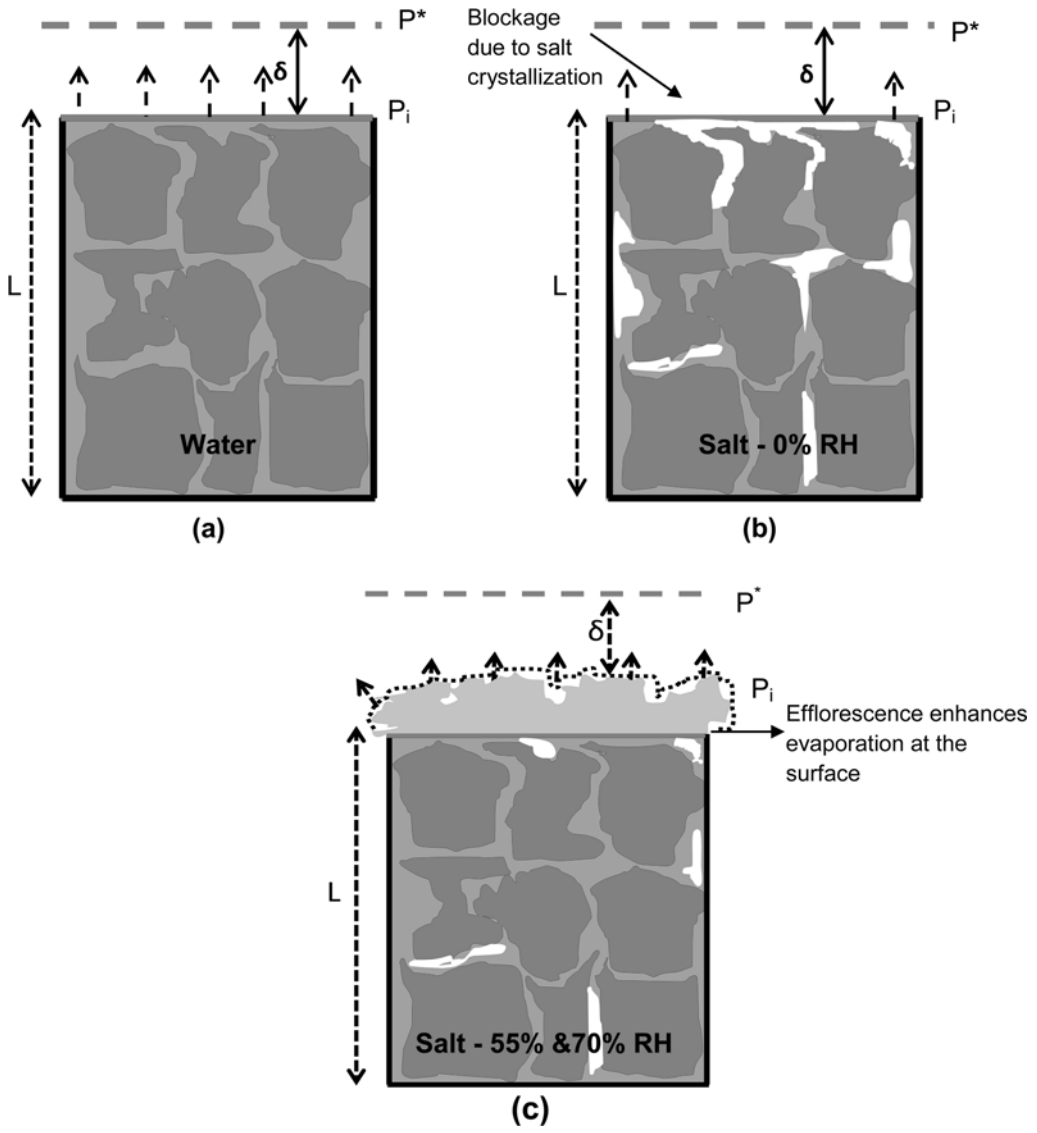

Figure 6. A schematic representation of the drying process for (a) water saturated brick, (b) salt saturated brick dried at 0% RH, and (c) salt saturated bricks dried at 55% and 70% RH. L is the length of sample, δ (m) is the thickness of air boundary layer through which the water vapor diffusion takes place, and P_i and P^* are the water vapor pressure at air/water interface at the material surface and in the surrounding air respectively. The number of arrows at the surface indicates the intensity of evaporative flux.

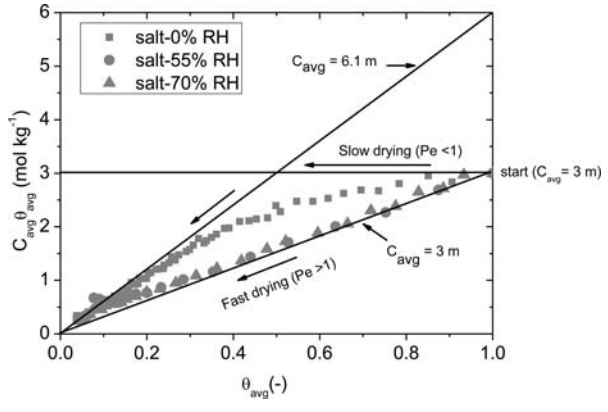

Figure 7. Efflorescence pathway diagram for salt saturated brick dried under different RH conditions. The data for 0% RH sample have been taken from a previously published article.[8] The total amount of dissolved sodium is plotted as a function of the average moisture content (θ_{avg}) in the brick.

between Pe < 1 and Pe > 1, that was followed at 0% RH. Thus, at high humidity, advection was the governing process, and ions were transported along with the moisture toward the outer surface of brick. This salt was observed at the end of the experiment as efflorescence. Because of the formation of efflorescence, the average salt ion concentration remained below saturation for a longer time compared to the brick dried at 0% RH. Also, at high humidity the dissolved salt ion concentration remained almost constant at about the starting concentration, that is, 3 m. However, near the end of the drying, where θ_{avg} (average moisture content inside the brick at a given time) was approximately 0.3, drying becomes slower, and a pathway in between the two extreme situations is followed, which ultimately ends on the Pe < 1 pathway. This indicates that near the end of the drying diffusion becomes dominant. This is caused by the penetration of a receding drying front. Because of this, drying becomes so slow that back diffusion of salt ions dominates. At this time approximately 30–40% of the initially dissolved salt was still present inside the

dx.doi.org/10.1021/cg4015459 | Cryst. Growth Des. 2014, 14, 1591–1599

brick and that cannot be transported to crystallize as efflorescence.

4.3. Drying Behavior of Salt Saturated Fired-Clay Brick with Inhibitor. To explore the influence of inhibitor on the drying and crystallization behavior of NaCl at different humidity conditions, the drying experiments were performed on salt saturated bricks containing inhibitor.

Drying Behavior of Salt + Inhibitor Saturated Fired-Clay Brick at 0% Relative Humidity. The drying behavior of water, salt and salt + inhibitor solution has been studied and compared. The results are shown in Figure 8, where the

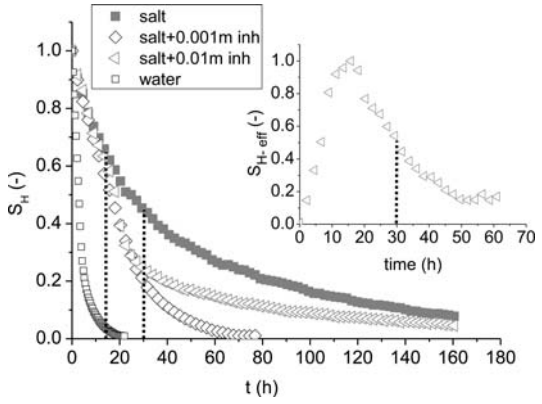

Figure 8. Normalized integrated hydrogen signal (S_H) as a function of time (t) for water and salt loaded bricks with and without inhibitor dried at 0% relative humidity. The integrated hydrogen signal has been calculated from the moisture profile data shown in our previous work.[8] In the inset, the hydrogen signal from the efflorescence ($S_{H\text{-}eff}$) formed on the outer surface of the brick (in the case of 0.01 m inhibitor) is plotted as a function of time.

normalized integrated hydrogen signal is plotted as a function of time. The moisture profiles of these samples have been shown elsewhere.[8] In this work, a detailed comparison of the drying behavior will be discussed. Two concentrations of inhibitor were tested, that is, 0.001 and 0.01 m.[16] Three main observations can be made. First, in the presence of inhibitor the initial drying rates of salt and salt + inhibitor saturated materials were similar. Second, after approximately 15 h a dramatic decrease in the drying rate of the salt saturated material without inhibitor was observed. However, in the presence of inhibitor at this time no drop in the drying rate was seen. Third, in the presence of 0.01 m inhibitor after approximately 25 h a dramatic decrease in the drying rate occurred. No such drop in flux was seen in the case of 0.001 m inhibitor.

The initial drying behavior of the systems with and without inhibitor was the same. This is caused by the fact that with the addition of inhibitor the equilibrium relative humidity of salt solution does not change. Therefore, the humidity gradient and hence the evaporative fluxes remain the same. The rate of initial volume change of the solution in various samples is plotted in Figure 5. This figure shows that, at 0% RH, initially the volume change with and without inhibitor is approximately the same. Even in the presence of inhibitor the values are much lower than expected on basis of the humidity gradient. This is attributed to the formation of a thin layer of salt crystals near the surface of the material which has a low permeability, as was expected to be formed in the case of salt saturated bricks without inhibitor (see section 4.2). For such a case, the initial drying behavior of the material with and without inhibitor should be the same. This has been confirmed by performing a droplet drying experiment (for the details of the experimental procedure see ref 8). The brick powder was added (as nucleation sites) to a salt solution droplet containing inhibitor. This droplet was dried inside the NMR setup simultaneously measuring the H and Na signal. In the presence of these external nucleation sites the onset of crystallization was observed at the saturation concentration (6.14 m), and thus no supersaturation occurred. This is different from the high supersaturation that has been reported, when a salt solution droplet containing inhibitor was dried without brick powder.[8] This indicates that NaCl solution will not supersaturate in most practical situations.

No drop in the drying rate was seen in the presence of inhibitor contrary to what was observed in the absence of inhibitor. In the absence of inhibitor after approximately 15 h, the saturation concentration was achieved in the top few millimeters of the sample (confirmed from the measured concentration profiles (for details see ref 8). Since most of the salt crystallized as subflorescence, it causes a more severe blockage of the pores near the drying surface. However, in the presence of inhibitor the crystal morphology changes from cubic to dendritic.[8] The salt solution creeps along the branches of the dendrites and transports more and more dissolved salt ions toward the drying surface to crystallize as efflorescence observed at the end of the drying experiment. Pictures of the materials with efflorescence are shown in Figure 3b,c. Approximately 26% and 69% of the salt crystallized as efflorescence in the presence of 0.001 and 0.01 m inhibitor respectively. These results are included in Figure 4. Because of the formation of efflorescence in the presence of inhibitor, the average salt ion concentration inside the brick remained below saturation. Therefore, the system remained open compared to the salt saturated system without inhibitor.

An extremely low drying rate was seen at later stages of drying (t > 30 h) in the case of 0.01 m inhibitor (see Figure 8). This is attributed to drying out of the efflorescence at the end of the drying process. In the inset of Figure 8, the hydrogen signal from the efflorescence formed on the outer surface of the brick (in case of 0.01 m inhibitor) is plotted as a function of time. This inset shows that initially, the hydrogen signal increases indicating the growth of the efflorescence. Note that the hydrogen signal comes from the water present in and on the efflorescence. After approximately 30 h (the time after which drying became extremely slow), the hydrogen signal from the efflorescence dropped significantly, indicating that the efflorescence was drying out. Dry efflorescence acts as a water vapor diffusion barrier, slowing down the drying process. Our results are in line with the observations made by previous authors.[17] At a lower concentration of inhibitor (0.001 m), no such dramatic drop in the drying rate was seen as the thickness of the efflorescence was much smaller.

Crystallization Behavior for Salt + Inhibitor Saturated Fired-Clay Brick Dried at 0% RH. To obtain the information about moisture/ion transport phenomena and salt crystallization processes inside the material, the crystallization behavior of salt + inhibitor saturated brick was plotted in an EPD (for details see ref 8). In the presence of inhibitor, advection was the governing process during drying. This promotes salt crystallization out of the brick as efflorescence. Thus, inside the brick saturation concentration was not attained for a longer period of time.[8]

dx.doi.org/10.1021/cg4015459 | Cryst. Growth Des. 2014, 14, 1591−1599

Drying Behavior of Salt + Inhibitor Saturated Fired-Clay Brick at 55% and 70% Relative Humidity. In practice the humidity is much higher than 0%, so the drying behavior of salt + inhibitor saturated brick was studied at higher humidity. The results for salt + inhibitor saturated brick dried at 55% and 70% RH are shown in Figure 9, panels a and b, respectively, where

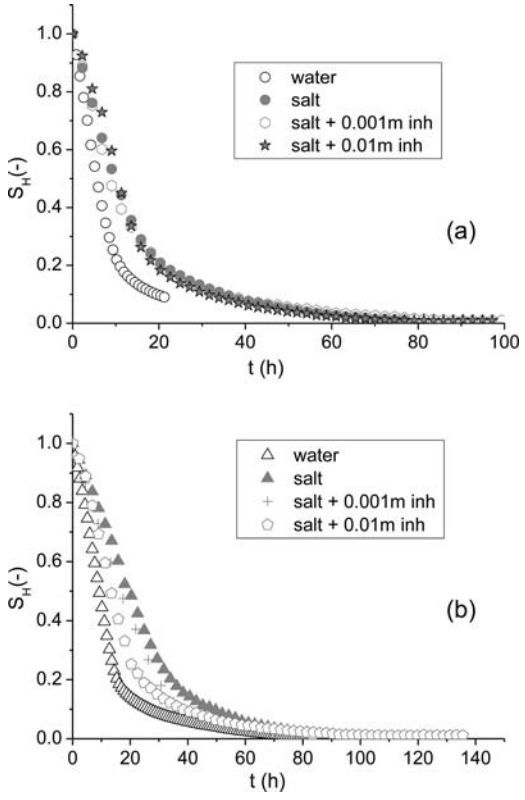

Figure 9. Normalized integrated hydrogen signal (S_H) as a function of time (t) for salt loaded bricks with and without inhibitor dried at (a) 55% relative humidity and (b) 70% relative humidity.

the normalized integrated hydrogen signal is plotted as a function of time. At higher relative humidity, no significant difference in the drying behavior of brick with and without inhibitor was seen. A comparable efflorescence was formed for both cases with and without inhibitor. The lower drying rate of salt and salt + inhibitor saturated bricks compared to water saturated brick at high humidity results from the depression of the humidity gradient. After correcting for this effect, the curves coincide rather well, similar to the case of salt saturated brick (see Figure 2b).

The drying behavior of the materials with and without inhibitor at high humidity was about the same. The values of the initial volume change for salt saturated material in the presence of inhibitor have been included in Figure 5. These values are close to the expected values of the drying rates. This is caused by the fact that at high humidity conditions for salt saturated materials the drying front is located at the surface of the material. Therefore, salt crystallizes as efflorescence. Because of the formation of efflorescence the system remains open, and no prominent blockage of pores near the drying surface is expected. As the system remains open, it extracts more dissolved salt ions out of the material to crystallize as efflorescence. The addition of inhibitor does not alter this situation.

Since the evaporative flux is same for the bricks with and without inhibitor, the velocity of the salt solution should also be the same, and about the same amount of efflorescence is expected for both cases. This indeed is observed at the end of drying experiment. Figure 3d–f shows the pictures of efflorescence for brick dried at 55% relative humidity. Approximately 48% of salt without inhibitor and 60% of salt with inhibitor crystallized as efflorescence. Figure 3g–i shows the pictures of efflorescence for brick dried at 70% relative humidity. Approximately 40% of salt without inhibitor and 60% of salt with inhibitor crystallized as efflorescence (see Figure 4).

Crystallization Behavior for Salt + Inhibitor Saturated Fired-Clay Brick Dried at 55% and 70% RH. To understand the salt crystallization processes inside the materials at higher humidity, the data are plotted in an EPD. The results are shown in Figure 10a,b for salt saturated bricks with and without

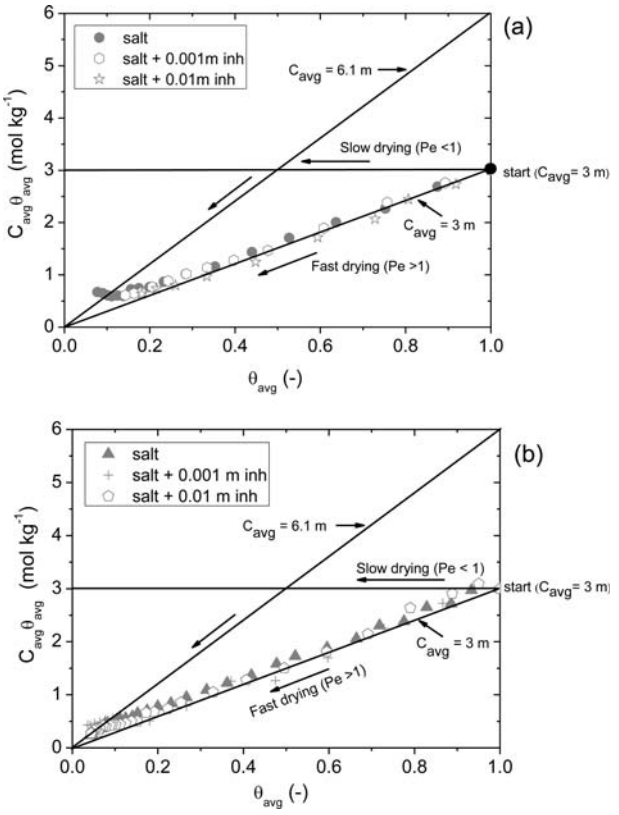

Figure 10. Efflorescence pathway diagram for salt saturated brick with and without inhibitor dried at (a) 55% RH and (b) 70% RH. The total amount of dissolved sodium ($C_{avg}\theta_{avg}$) is plotted as a function of the average moisture content (θ_{avg}) in the brick.

inhibitor dried at 55% and 70% RH respectively. The behavior of salt saturated brick without inhibitor has already been discussed in section 4.2. For the materials with inhibitor, advection remained the governing process throughout the drying process. In the presence of inhibitor, the sodium content decreased at the same rate as without inhibitor, and therefore salt crystallization was delayed for the same amount of time. Addition of inhibitor causes no delay in attaining the saturation concentration inside the brick. Toward the end of the drying process (approximately near θ_{avg} = 0.3), diffusion started to be dominant because of the penetration of a receding drying front. Therefore, after this time no more salt can be transported toward the outer surface of brick to crystallize as efflorescence.

dx.doi.org/10.1021/cg4015459 | *Cryst. Growth Des.* 2014, 14, 1591–1599

5. CONCLUSIONS

Drying of a salt loaded fired-clay brick is faster at high humidity than at low humidity. This is caused by the fact that at low humidity, advection is so dominant in the initial stage of drying process and that ions quickly crystallize and block the surface. At a later stage of the drying, back diffusion of ions dominates which levels off the salt ion concentration inside the brick. This causes the salt to crystallize inside the brick as subflorescence. At high humidity, salt crystallizes outside the material as efflorescence. This prevents blockage of the pores, thereby keeping the system open to transport more and more salt outside the material. Advection remains the governing process for ion transport, and no drop in the drying rate is seen. Addition of inhibitor was found to be useful at low humidity conditions. At low humidity, due to distinct crystal morphology in the presence of inhibitor salt crystallizes as nondestructive efflorescence. This prevents a severe blockage as was seen for salt loaded material at low humidity.

At high humidity conditions, addition of inhibitor to the salt loaded bricks had no significant effect on the drying behavior, the amount of efflorescence formed, the moisture and ion transport, and the salt concentration levels attained inside the brick. This is caused by the fact that because of the slow dying at high humidity, the salt ions crystallize outside the material as nondestructive efflorescence. Consequently, the system remains open and the addition of inhibitor has no effect.

This study helps to understand that the success of adding an inhibitor strongly depends on the local climate. The effect of inhibitor on the sheltered areas of a monument would be different from that on the areas exposed to sun and wind. Before using inhibitor in practice, these aspects should be considered carefully.

■ AUTHOR INFORMATION

Corresponding Author

*Tel.: +31 40 247 5375. Fax: +31 40 243 2598. E-mail: h.p.huinink@tue.nl.

Notes

The authors declare no competing financial interest.

■ ACKNOWLEDGMENTS

We thank Hans Dalderop and Jef Noijen for their technical assistance. A part of this project is supported by the Dutch technology foundation (STW).

■ REFERENCES

(1) Scherer, G. W. *Cem. Concr. Res.* **1999**, *29*, 1347−1358.
(2) Sangwal, K. J. *J. Cryst. Growth* **1993**, *128*, 1236−1244.
(3) Sangwal, K. *Prog. Cryst. Growth Charact. Mater.* **1998**, *36*, 163−248.
(4) Navarro, C. R.; Fernandez, L. L.; Doehne, E.; Sebastian, E. *J. Cryst. Growth* **2002**, *243*, 503−516.
(5) Lubelli, B.; Van Hees, R. P. J. *J. Cult. Herit* **2007**, *8*, 223−234.
(6) Veran-Tissoires, S.; Marcoux, M.; Prat, M. *Phys. Rev. Lett.* **2012**, *108*, 054502.
(7) Eloukabi, H.; Sghaier, N.; Ben Nasrallah, S.; Prat, M. J. *Heat Mass Transfer* **2013**, *56*, 80−93.
(8) Gupta, S.; Terheiden, K.; Pel, L.; Sawdy, A. *Cryst. Growth Des.* **2012**, *12* (8), 3888−3898.
(9) Steiger, M. *J. Cryst. Growth* **2005**, *282*, 470−481.
(10) Kopinga, K.; Pel, L. *Rev. Sci. Instrum.* **1994**, *65*, 3673−3681.
(11) Espinosa-Marzal, R. M.; Scherer, G. W. *Environ. Geo.* **2008**, *56*, 605−621.
(12) Hamilton, A.; Hall, C.; Pel, L. J. *Phys. D: Appl. Phys.* **2008**, *41*, 212002/1−212002/5.
(13) Schiro, M.; Ruiz-Agudo, E.; Rodriguez-Navarro, C. *Phys. Rev. Lett.* **2012**, *109* (26), 26550/1−26550/5.
(14) Huinink, H. P.; Pel, L.; Michels, M. A. *J. Phys. Fluids* **2002**, *14*, 1389−1395.
(15) Pel, L.; Huinink, H. P.; Kopinga, K. *Appl. Phys. Lett.* **2002**, *81*, 2893−2895.
(16) Gupta, S.; Pel, L.; Sawdy, A. *Proceedings of 12th International Congress on the Deterioration and Conservation of Stone*, New York, October 22−26, 2012; International Institute for Conservation of Historic and Artistic Works: London.
(17) Sghaier, N.; Prat, M. *Transp. Porous Med.* **2009**, *80*, 441−454.